Failure Control of an Electric Transmission Tower System under Strong Earthquakes

Nazim Abdul Nariman[1] & Ilham Ibrahim Mohammad[2] & Glena Nooraddin[3] & Tavi Simko[4]

[1,2,3&4] Department of Civil Engineering, Tishk International University-Sulaimani, Sulaimaniya, Iraq
Correspondence: Nazim Abdul Nariman, Tishk International University- Sulaimani, Sulaimaniya, Iraq.
Email: nazim.abdul@tiu.edu.iq

Doi: 10.23918/eajse.v8i1p101

Abstract: The aim of the project is to control the failure of the structural system of an electric transmission tower system during strong earthquakes. Optimization process is being applied by the support of both surrogate modeling and Hessian Matrix method using MATLAB codes. Latin Hypercube sampling method is dedicated to arrange twenty-five numerical models of the system in ABAQUS program. Five parameters are used in the optimization process which are the thickness of steel member of the transmission tower, the Modulus of Elasticity of the steel member, radius of the conductor steel wire, Modulus of Elasticity of the conductor steel wire, and the Peak ground acceleration of the earthquake. The first four parameters are controllable in the design but the last parameter is can't be controlled because it is uncertain and it is related to the earthquake strength. The surrogate models for the maximum principal stress and maximum principal strain of the structural system are constructed. The coefficients of determination of both surrogate models were 97.02% and 92.06% respectively, which are considered excellent and reliable for representing and predicting the responses of the structural system. The results of the optimization all involved five parameters from the Hessian Matrix method for both surrogate models were very accurate and are optimum values through comparing the responses of them in the surrogate models with the numerical simulation results. The surrogate modeling and the Hessian Matrix method are great tools which can be utilized in the optimization of the design of the electric transmission tower system under strong earthquakes. Consequently, the failure of the structural system then can be easily controlled to a great extent in the design stage and after construction.

Keywords: Conductor Wire, Latin Hypercube Method, Surrogate Model, Hessian Matrix Method, Maximum Principal Strain, Maximum Principal Stress

1. Introduction

Power transmission tower-line system is a critical component of a power system. Its failure may result in the shutdown of the power supply. Static load, wind loads, ice load, impulsive load, and other factors are considered while designing a transmission tower. However, most transmission lines in China must pass a high seismic intensity zone. Previous earthquakes have harmed numerous towers and wires and resulted in large financial damage. Several towers were destroyed in the Tangshan earthquake of 1976, about 38 transmission lines were harmed and 20 towers were slanted as a result of foundation movement during the 1995 Kobe earthquake, many wires were severed and some towers were destroyed during the 1999 Chi-Chi earthquake. The Sichuan power network was severely damaged in the 2008 Wenchuan earthquake. And during the 2013 Yaan earthquake in China, electric systems were

Received: April 2, 2022
Accepted: May 28, 2022
Nariman, N.A., & Mohammad, I.I., Nooraddin, G., & Simko, T. (2022). Failure Control of an Electric Transmission Tower System under Strong Earthquakes. *Eurasian Journal of Science and Engineering*, *8*(1), 101-118.

harmed (Walid et al., 2016). Transmission line failure during a typhoon or storm can paralyze the electrical grid, affecting following construction, living quality, and emergency relief directly and potentially creating catastrophic secondary crises. Several transmission lines have already collapsed due to strong gales and thunderstorms. To guarantee the safe functioning of the power grid, it is critical to investigate the strength capacity of transmission towers during heavy winds and describe the breakdown modes (Richardson, 1975). Several recent cases of transmission tower harm during earthquakes have been mentioned, for example, during the 1994 Northridge earthquake, two transmission towers slumped due to large ground movement, and during the 1999 Chi-Chi earthquake, a large number of electric power transmission towers suffered serious structural issues. During the 1999 Chi-Chi earthquake, damage to electric power transmission towers resulted in blackouts in Taiwan's central and northern areas. Telephone connectivity, both wired and wireless, was also disrupted, and it took 36 hours for it to be restored (Larsen & Gimsing, 1992). Despite it, the transmission tower appears to be vulnerable to strong earthquakes (Miyata, 2003). Transmission towers, which are high structures, should have lateral displacement limited to tolerable levels under seismic stresses. To demonstrate appropriate earthquake management, it is critical to have a thorough awareness of the transmission tower's seismic vulnerability (Larsen & Larose, 2005). The main objective is to gain a better knowledge of how lattice steel transmission towers operate under earthquake loads. A transmission steel tower, also known as an electricity tower, is a high-rise building. It is used to convey overhead power lines (Wang et al., 2012). Advances in electrical engineering have revealed the necessity to sustain heavy conductors, resulting in the current towers. Transmission line towers are tall buildings with a height that exceeds the side dimensions. These are steel-profiled space frames with individual foundations for each leg. The transmission tower's elevation is determined by the client, and the general layout, element, and connecting details are designed by the engineer. As a result, the weight of the tower, the tension in the transmission cable, and the wind load are all taken into account when determining the cross-section of structural components. Despite that, the transmission tower appears to be vulnerable to strong earthquakes (Diana et al., 2013). Standard seismic analysis of transmission towers usually considers each tower as an independent structure, ignoring the strong traction provided by high-voltage electrical cables lined up in numerous directions in the air.

Furthermore, in seismic analysis, many structural engineers used to simply disregard the wire mass or treat the wire mass as a combined mass associated with the tower. The results of such analytical schemes would be unable to accurately represent the true forced situations of the tower structure and the base foundation underneath it (Meng et al., 2011). Most of the study has concentrated on the impacts of static, impulsive, and comparable static wind forces. In existing seismic codes, there are no calculation techniques for considering transmission line constructions under earthquake stress (Tang et al., 2021: Sham & Wyatt, 2016). Many nonlinear issues, including dynamic nonlinearity, geometric nonlinearity, and material nonlinearity, are involved in the seismic dynamic responses of transmission towers (Khuri & Mukhopadhyay, 2010).

Moon et al. (2019) used semi-scaled substructure data to assess the behavior and fault location of an existing transmission tower that was subjected to wind forces. Local regional buckling happened on the two legs components where they had been compressed, according to the results of the experiment. The elements must be expanded or braces placed to weak joints to avoid associated regional buckling and uneven deformation. Alam & Santhakumar, (1996) conducted a load test on a 34-meter high transmission tower with a capacity of 200 kV. The entire bending of the tower legs and transverse components was revealed to be the reason for the tower's failure. According to the conclusions of the

testing, the maximal slenderness ratio of 150 should be reduced to 110, as indicated in the steel transmission tower design code (American Society of Civil Engineers, 1971). Li et al. (2017) in the study of progressive collapse has practical clues for transmission tower-line systems with long spans. The Tian–Ma–Qu model is used to capture the nonlinear behaviors of elements when considering material damage impact. The damage index is chosen as the element's failure criteria. In ABAQUS, a three-dimensional finite element model of steel-latticed towers supporting transmission lines is built. Based on the site circumstances, 7 seismic records are chosen and edited to match the needed design spectrum. The collapse process of the El Centro long-span transmission tower-line system is explored, and an incremental dynamic analysis is performed to determine the structure's collapse resistance capability. The amplification factor is offered as a way to assess the structure's ability to withstand collapse. Intersegment displacement ratio results are used to investigate the displacement reactions of electricity transmission towers. The results of the research can be used as a guide for the seismic design of long-span transmission tower-line systems. Xiaohong et al. (2018) state that transmission tower collapses are complicated by a number of problems, including member failure, geometric, material, and dynamic nonlinearity. The traditional finite element method (FEM), which is based on the continuum and variation principles, makes simulation of the collapse process problematic, but the finite particle method (FPM) guarantees equilibrium at each site. The ability of particles to split from one another is beneficial when simulating structure collapse. The finite particle method (FPM) is used in this paper to model the collapse of a transmission steel tower due to seismic ground movement; a three-dimensional (3D) finite particle model using MATLAB and a three-dimensional (3D) finite element model using ANSYS of the transmission steel tower are created, respectively. The static and elastic seismic response analyses show that the FPM's results are consistent with the FEM's. A failure criterion based on the ideal elastic-plastic model and a failure mode is proposed to simulate the collapse of the transmission steel tower. Finally, utilizing the finite particle method, the collapse simulation of transmission steel towers exposed to unidirectional earthquake ground motion and the collapse seismic fragility analysis can be successfully completed. The transmission steel tower has a greater seismic safety and anti-collapse ability, according to the findings.

The main objective of this study is to control the failure of the transmission tower system under earthquakes by predicting the response of the system through the use of surrogate models by considering five parameters. The parameters are related to the material properties of both steel sections and conductor wires. The surrogate models are created using Latin Hypercube sampling methods to generate 25 models of the transmission tower system in ABAQUS finite element program.

2. Equation of Motion

The equilibrium equation of motion may be stated as follows when considering differential seismic movements at distinct tower supports:

$$\begin{bmatrix} M_{ss} & M_{sb} \\ \mathrm{M}_{\mathrm{sb}}^{\mathrm{T}} & M_{bb} \end{bmatrix} \begin{bmatrix} \ddot{\mathrm{X}}_s \\ \ddot{\mathrm{X}}_b \end{bmatrix} + \begin{bmatrix} C_{ss} & C_{sb} \\ \mathrm{C}_{\mathrm{sb}}^{\mathrm{T}} & C_{bb} \end{bmatrix} \begin{bmatrix} \dot{\mathrm{X}}_s \\ \dot{\mathrm{X}}_b \end{bmatrix} + \begin{bmatrix} K_{ss} & K_{sb} \\ \mathrm{K}_{\mathrm{sb}}^{\mathrm{T}} & K_{bb} \end{bmatrix} \begin{bmatrix} \mathrm{X}_s \\ \mathrm{X}_b \end{bmatrix} = \begin{Bmatrix} O \\ P_b \end{Bmatrix} \quad [1]$$

The mass matrix, the viscous damping matrix, and the stiffness matrix, respectively, are M, C, and K. The structural, support, and coupled DOFs are denoted by the subscripts ‘ss', ‘bb', and ‘sb', accordingly. The acceleration vector, velocity vector, and displacement vector are represented as Ẍ, Ẋ, and X sequentially. The sustaining force vector is denoted by the letter P. The letters 's' and 'b' stand

for structure and base, respectively. The equilibrium equation describing the response DOFs of the superstructure may be obtained from as follows:

$$M_{ss}\ddot{\mathrm{X}}_s + C_{ss}\dot{\mathrm{X}}_s + K_{ss}\mathrm{X}_s = -M_{sb}\ddot{\mathrm{X}}_b - C_{sb}\dot{\mathrm{X}}_b - K_{sb}\mathrm{X}_b \quad [2]$$

We can get Msb =0 and Csb =0 by assuming the lumped mass and ignoring the cross damping coefficients between the structure and the base DOFs. Eq. (2) is thus simplified to Eq. (3) (Meng et al., 2011):

$$M_{ss}\ddot{\mathrm{X}}_s + C_{ss}\dot{\mathrm{X}}_s + K_{ss}\mathrm{X}_s = -K_{sb}\mathrm{X}_b \quad [3]$$

3. Response Surface Model

A response surface model (RSM) is a collection of statistical and mathematical techniques that are useful for developing, improving, and optimizing processes. The choice of RSM for a given computational model depends on the knowledge of the computational model itself (Myers et al., 2016: Kwak, 2005). It is used in the development of an adequate functional relationship between a response of interest $\boldsymbol{y}$, and a number of associated input parameters denoted by (x1, x2, . . . , xk). In general, such a relationship is unknown but can be approximated by a low-degree polynomial model of the form:

$$y = f(x)\beta + \epsilon \quad [4]$$

where $\boldsymbol{x}$ = (x1, x2, . . . , xk) , f (x) is a vector function of p elements that consists of powers and cross-products of powers of x1, x2, . . . , xk up to a certain degree denoted by d (≥ 1), β is a vector of p unknown constant coefficients referred to as parameters, and ϵ is a random experimental error assumed to have a zero mean. This is conditioned on considering the model provides an adequate representation of the response. In this case, the quantity $\boldsymbol{f'(x)\beta}$ represents the mean response, that is, the expected value of y, and is denoted by μ(x). Two important models are commonly used in RSM. These are special cases of model in Eq. (4) and include the first-degree model (d = 1):

$$y = \beta_o + \sum_{i=1}^{k} \beta_i x_i + \epsilon \quad [5]$$

And the second-degree model (d = 2)

$$y = \beta_o + \sum_{i=1}^{k} \beta_i x_i + \sum_{i<j} \sum \beta_{ij} x_i x_j + \sum_{i=1}^{k} \beta_{ii} x^2{}_i + \epsilon \quad [6]$$

A series of n experiments should first be carried out, in each of which the response $\boldsymbol{y}$ is measured (or observed) for specified settings of the control parameters. The totality of these settings constitutes the so-called response surface design, or just design, which can be represented by a matrix, denoted by D, of order n × k called the design matrix,

$$D = \begin{pmatrix} x_{11} & x_{12} & . & . & . & x_{1k} \\ x_{21} & x_{22} & . & . & . & x_{2k} \\ . & . & . & . & . & . \\ . & . & . & . & . & . \\ . & . & . & . & . & . \\ x_{n1} & x_{n2} & . & . & . & x_{nk} \end{pmatrix} \quad [7]$$

Where x_{ui} denotes the uth design setting of $\boldsymbol{x_i}$ (i = 1, 2, . . . , k; u = 1, 2, . . . , n). Each row of D represents a point, referred to as a design point, in a k-dimensional Euclidean space. Let $\boldsymbol{y_u}$ denote the response value obtained as a result of applying the u th setting of x, namely $\boldsymbol{x_u} = (x_{u1}, x_{u2}, \ldots, x_{uk})$, (u = 1, 2, . . . , n). From Eq. (4), we then have:

$$y_u = f'(x_u)\beta + \epsilon_u \ , \ \ u = 1,2, \ldots . , n \quad [8]$$

Where $\boldsymbol{\epsilon_u}$ denotes the error term at the u th experimental run. Eq. (8) can be expressed in matrix form as:

$$y = X\beta + \epsilon \quad [9]$$

where $\boldsymbol{y}$= ($y1$, $y2$, . . . , yn) , $\boldsymbol{X}$ is a matrix of order n × p whose u th row is $\boldsymbol{f'(x_u)}$, and $\boldsymbol{\epsilon}$ = ($\epsilon 1$, $\epsilon 2$, . . . , ϵn). Note that the first column of $\boldsymbol{X}$ is the column of ones 1n. Assuming that $\boldsymbol{\epsilon}$ has a zero mean, the so-called ordinary least-squares estimator of β is (Khuri & Mukhopadhyay, 2010):

$$\hat{\beta} = (X'X)^{-1} X'y \quad [10]$$

4. Surrogate Models

The surrogate models are created using MATLAB codes to determine the coefficients of regression for each response. The least-square method will be adopted to formulate two surrogate models. The design matrix is generated to help to formulate the surrogate models by entering the least-square method equation.

The regression analysis is necessary to compare the results gained from the experimental tests and the results predicted by the surrogate models. Coefficient of determination R2 is a tool used to identify the efficiency of the surrogate models, where this parameter has a range value starting from 0 to 1. This parameter is making use of a comparison between the experimental test results and the predicted results. When the value of this parameter is near 1 it means that the surrogate models are efficient and can be supported on to predict the responses of any structural system.

5. Finite Element Model

The steel transmission tower is modeled in ABAQUS finite element program as a system of three transmission tower with eight lines of steel conductor wires see Figure 1. The transmission tower is 93 m height, 24 m length and 24 m width. The tower consists of steel angle sections connected in fixed joints see Figure 2. The distance between the transmission towers is 150 m. The conductor wires are each pre-stressed (tension) to the modeled position by a 5840 Pa. A dynamic implicit step consisting of a high amplitude earthquake for the duration of 14 seconds is applied on the transmission tower

system. The transmission tower and the conductor wires are both meshed with 3294 elements of B32: A 3- node standard quadratic beam in space.

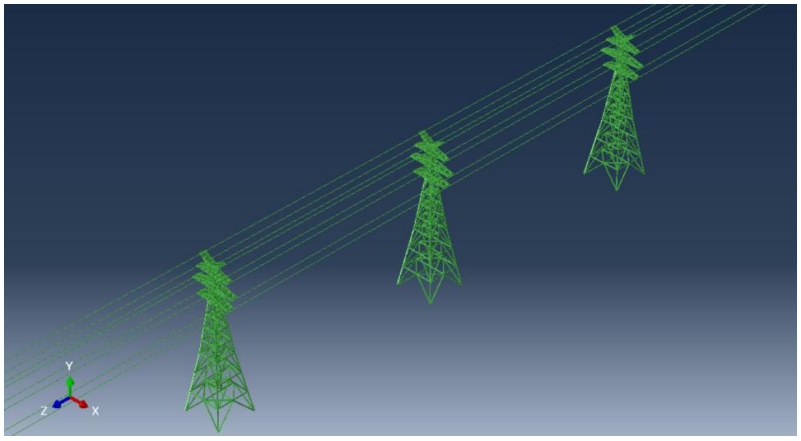

Figure 1: Transmission towers system with conductor wires

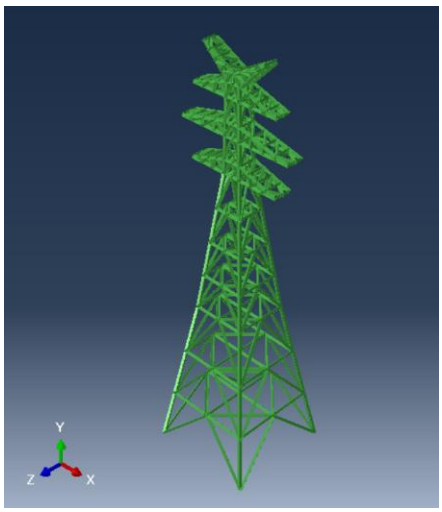

Figure 2: A transmission tower - rendered 3 times

5.1 Material Data Variation

The surrogate modeling which is the important part for the optimization step, needs to arrange the adopted five parameters supporting on a certain experimental design method. The Latin Hypercube design experimental method has been utilized to determine the 25 models. The following Table 1 is showing the adopted parameters and the range of the values of them. Table 2 is authorizing the 25 models with different parameters values.

Table 1: Material ranges of parameters

Parameter	Material	Range
X_1	Thickness of Angle Section for Steel Member (m)	0.018 - 0.026
X_2	Modulus of Elasticity of Steel Member (GPa)	190 - 230
X_3	Radius of Conductor Wire (m)	0.019- 0.028
X_4	Modulus of Elasticity of Steel Wire (GPa)	70 - 82
X_5	Peak Ground Acceleration (m/s^2)	0.4 - 1.2

5.2 Model Arrangement - Latin Hypercube Method

The following Table 2 contains information about 25 models of the transmission tower. Each model has different parameter values. The models are being designed for the strong earthquake for the duration of 14 seconds.

Table 2: Models arrangement

Model	X_1	X_2	X_3	X_4	X_5
Model 1	0.023667	226.666667	0.01975	73.5	0.566667
Model 2	0.018667	201.666667	0.0205	78	0.466667
Model 3	0.025333	210	0.025375	77	0.633333
Model 4	0.025667	221.666667	0.0235	82	0.866667
Model 5	0.020667	193.333333	0.022	80.5	1
Model 6	0.023333	225	0.023125	75.5	0.933333
Model 7	0.02	195	0.028	81.5	0.8
Model 8	0.018	220	0.023875	75	0.7
Model 9	0.019667	223.333333	0.026125	76.5	1.166667
Model 10	0.022333	191.666667	0.02425	74	0.766667
Model 11	0.019	230	0.021625	74.5	1.033333
Model 12	0.026	215	0.0265	78.5	1.133333
Model 13	0.025	205	0.02125	81	1.066667
Model 14	0.018333	190	0.022375	72.5	0.733333
Model 15	0.023	228.333333	0.027625	80	0.966667

Model 16	0.024333	208.333333	0.020125	71	1.1
Model 17	0.021667	200	0.025	71.5	1.2
Model 18	0.024	203.333333	0.02275	70	0.6
Model 19	0.021333	218.333333	0.024625	79	0.533333
Model 20	0.024667	196.666667	0.019375	76	0.666667
Model 21	0.020333	211.666667	0.02575	73	0.433333
Model 22	0.021	216.666667	0.020875	79.5	0.833333
Model 23	0.022667	213.333333	0.02725	72	0.9
Model 24	0.022	198.333333	0.026875	77.5	0.4
Model 25	0.019333	206.666667	0.019	70.5	0.5

5.3 Earthquake Data

The earthquake data has been considered from the literature with modification. The ground motion has a duration of 14 seconds applied in ABAQUS in the transverse direction perpendicular on the longitudinal direction of the conductor wires. The amplitude of the ground motion of the earthquake is shown in Figure 3.

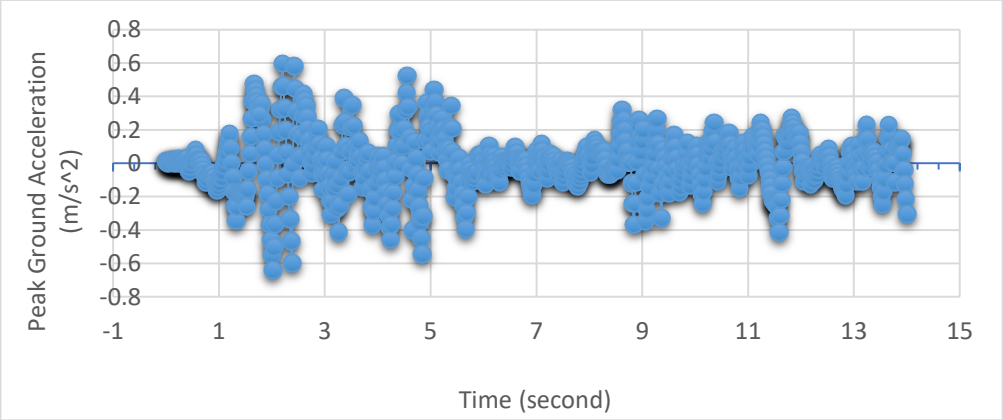

Figure 3: Ground motion data

6. Results and Discussion

6.1 Maximum Principal Strain

The results of the maximum principal strain for the 25 models of the transmission tower system under earthquake for 14 seconds are presented in both Table 3 and Figure 4. The maximum value of the maximum principal strain occurred in model 9 which was 0.00911 and the minimum value of the maximum principal strain can be seen in model 25 which is 0.002313. There is a random distribution

for the values of the maximum principal strain due to the distribution of Latin Hypercube sampling which has a non-regular distribution.

Table 3: 25 models - maximum principal strain

Model	Maximum Principal Strain ( )
Model 1	0.002893
Model 2	0.003085
Model 3	0.003769
Model 4	0.004432
Model 5	0.006864
Model 6	0.004552
Model 7	0.005139
Model 8	0.003915
Model 9	0.00911
Model 10	0.007096
Model 11	0.004989
Model 12	0.006819
Model 13	0.006259
Model 14	0.006527
Model 15	0.004783
Model 16	0.005839
Model 17	0.006278
Model 18	0.003896
Model 19	0.003124
Model 20	0.00505
Model 21	0.002444
Model 22	0.004523
Model 23	0.005287
Model 24	0.003413
Model 25	0.002313

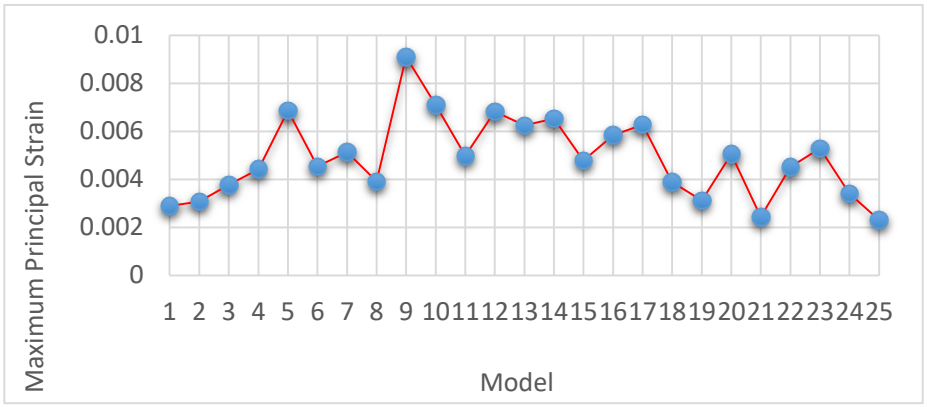

Figure 4: Maximum principal strain - 25 models

6.2 Maximum Principal Stress

In the same way, the results of the maximum principal stress for the 25 models of the transmission tower system are presented in both Table 4 and Figure 5. The maximum value of the maximum principal stress occurred in model 9 which was 1383000000 Pa and the minimum value of the maximum principal stress is obvious in model 21 which is 517400000 Pa. Also, a random distribution for the values of the maximum principal stress can be seen due to the distribution of Latin Hypercube sampling which has a non-regular distribution.

Table 4: 25 models - maximum principal stress

Model	Maximum Principal Stress (Pa)
Model 1	655700000
Model 2	622100000
Model 3	791500000
Model 4	982400000
Model 5	1290000000
Model 6	1024000000
Model 7	1002000000
Model 8	815400000
Model 9	1383000000
Model 10	1279000000
Model 11	1148000000
Model 12	1355000000
Model 13	1248000000
Model 14	1240000000
Model 15	1092000000
Model 16	1216000000

Model 17	1256000000
Model 18	792200000
Model 19	682100000
Model 20	993100000
Model 21	517400000
Model 22	980000000
Model 23	1128000000
Model 24	676900000
Model 25	569000000

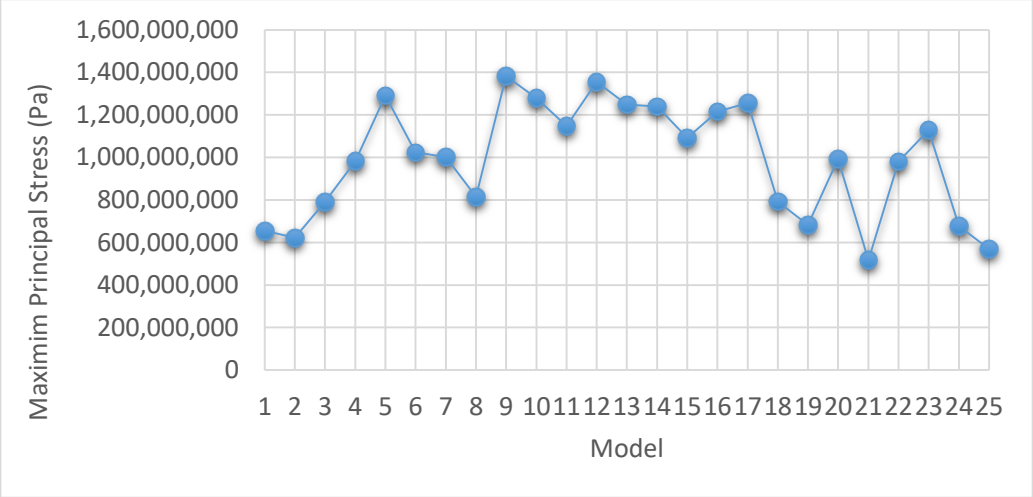

Figure 5: Maximum principal stress - 25 models

6.3 Simulation Results

The following figures manifest the positions and the magnitudes of the maximum principal strain and maximum principal stress in the transmission tower system for model 2, model 3, model 4 and model 5 which have been arbitrarily selected. For the model 2 the magnitudes of the maximum values for the maximum principal strain and maximum principal stress are 0.003085 and 622100000 Pa respectively which is occurring in one of the supports of the transmission tower see Figure 6.

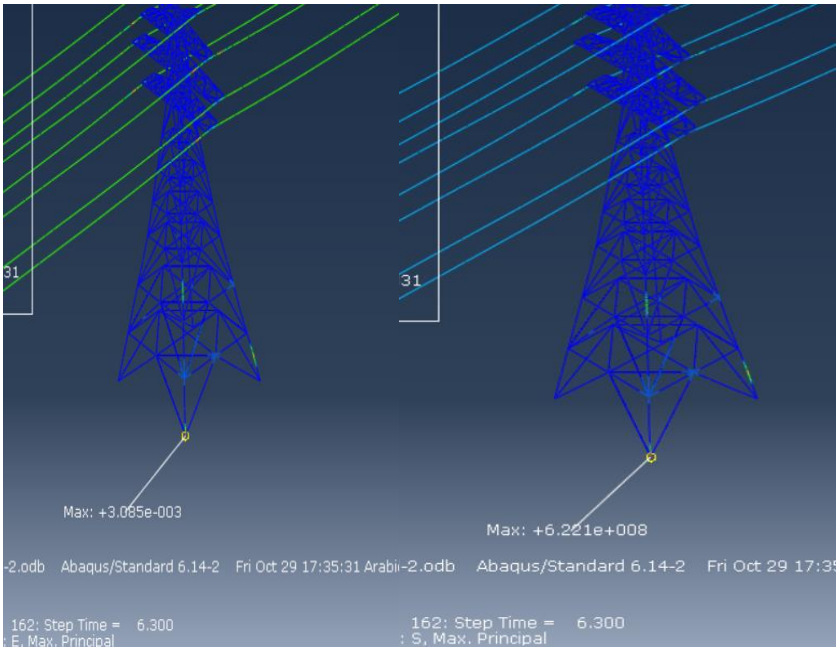

Figure 6: Maximum principal stress and maximum principal strain- model 2

For the model 3 the magnitudes of the maximum values for the maximum principal strain and maximum principal stress are 0.003769 and 791500000 Pa respectively which is occurring in one of the supports of the transmission tower see Figure 7.

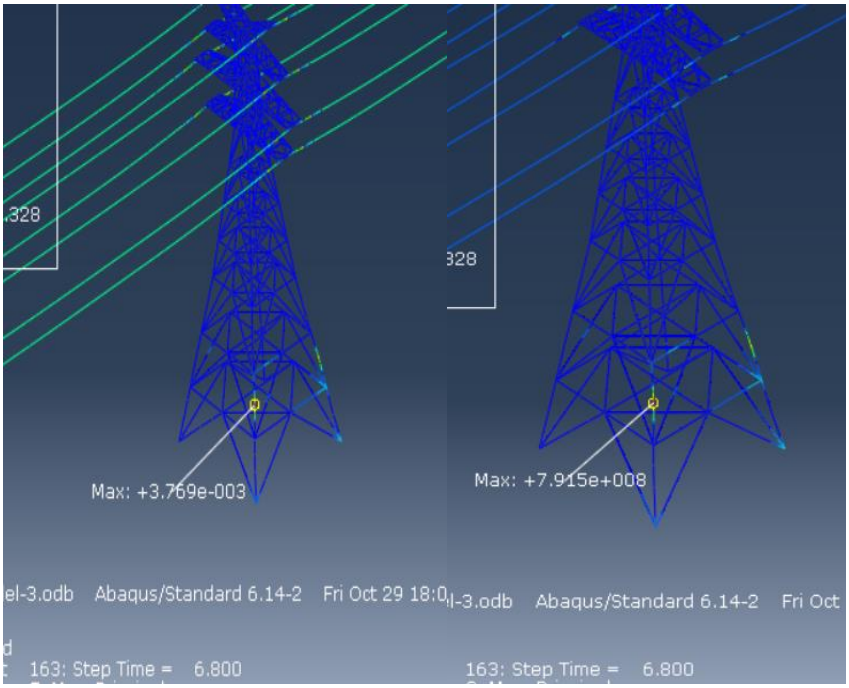

Figure 7: Maximum principal stress and maximum principal strain- model 3

For the model 4 the magnitudes of the maximum values for the maximum principal strain and maximum principal stress are 0.004432 and 982400000 Pa respectively which is occurring in one of the supports of the transmission tower see Figure 8.

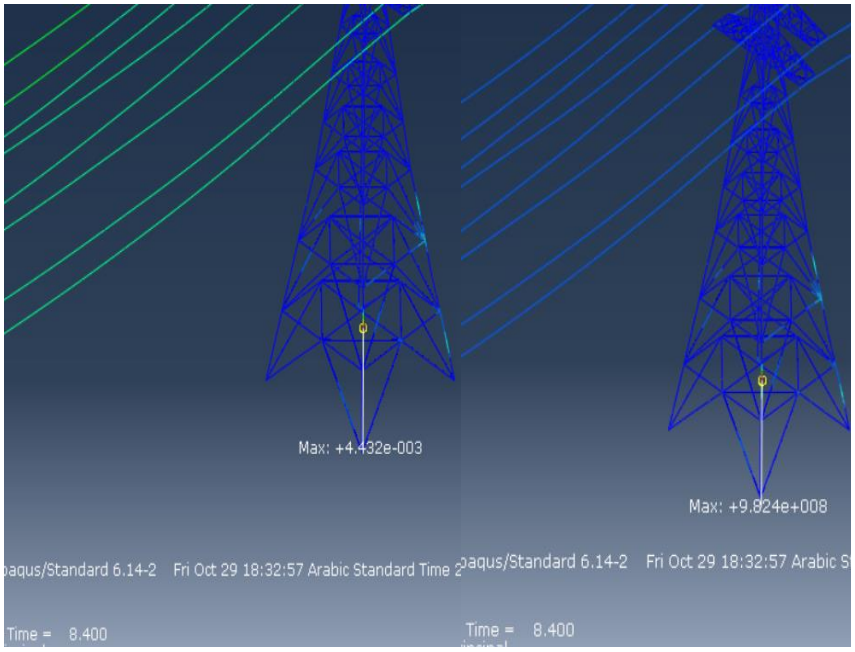

Figure 8: Maximum principal stress and maximum principal strain- model 4

For the model 5 the magnitudes of the maximum values for the maximum principal strain and maximum principal stress are 0.006864 and 1290000000 Pa respectively which is occurring in one of the supports of the transmission tower see Figure 9.

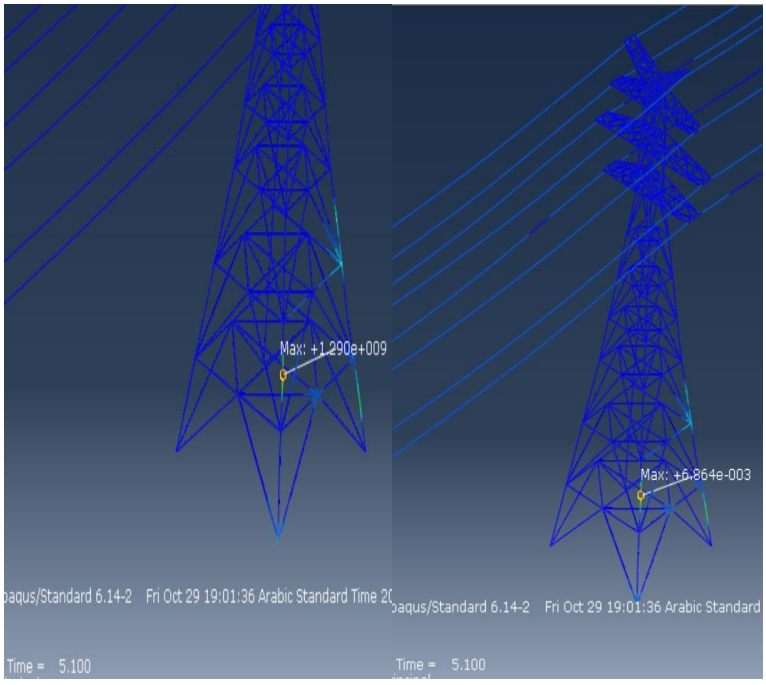

Figure 9: Maximum principal stress and maximum principal strain- model 5

6.4 Surrogate Models Results

The results of the surrogate models for the maximum principal stress and the maximum principal strain of the transmission tower during earthquakes have been determined by using the Latin Hypercube design sampling method and MATLAB codes. The least square method has been dedicated to determine the regression coefficients for the surrogate models (see Table 5). The regression coefficients are used to illustrate the final surrogate models for the responses of the transmission tower system due to the earthquakes.

The maximum principal stress has been expressed by MPSS and the maximum principal strain has been denoted by MPSN (see the following equations 11 and 12).

Table 5: Regression coefficients

Regression Coefficient	Maximum Principal Stress MPSS	Maximum Principal Strain MPSN
β_0	1231531227.990	-0.162489050218614
β_1	1508664351.237	0.889850725918118
β_2	-168999816.014	-0.000355295014225
β_3	132871184085.877	2.216778544907190
β_4	450635802.361	0.005042239572897
β_5	-2108305854.874	-0.046771152962135
β_{11}	618502285546.000	4.330941544606410
β_{22}	233413.594	-0.000000745656814
β_{33}	383817807051.189	-31.582143858444100
β_{44}	-3867067.878	-0.000041427857404
β_{55}	-525207831.767	0.000540239218776
β_{12}	220844296.572	0.006277898765933
β_{13}	-1079144922439.060	-53.349524139485800
β_{14}	-672762849.504	-0.012409597487409
β_{15}	5290037180.378	-0.340152093642835
β_{23}	-159111854.636	-0.000866340604559
β_{24}	725603.512	0.000005209576702
β_{25}	8934358.296	0.000115555146264
β_{34}	-1074562332.951	0.006095282897997
β_{35}	-10618065246.538	0.236764117677313
β_{45}	29945288.148	0.000395941759427

$$\text{MPSS} = 1231531227.990 + 1508664351.237 * X1 - 168999816.014 * X2 + 132871184085.877 * X3 + 450635802.361 * X4 - 2108305854.874 * X5 + 618502285546 * X1^2 + 233413.594 * X2^2 + 383817807051.189 * X3^2 - 3867067.878 * X4^2 - 525207831.767 * X5^2 + 220844296.572 * X1 * X2 - 1079144922439.060 * X1 * X3 - 672762849.504 * X1 * X4 + 5290037180.378 * X1 * X5 - 159111854.636 * X2 * X3 + 725603.512 * X2 * X4 + 8934358.296 * X2 * X5 - 1074562332.951 * X3 * X4 - 10618065246.538 * X3 * X5 + 29945288.148 * X4 * X5 \quad [11]$$

$$\text{MPSN} = -0.162489050218614 + 0.889850725918118 * X1 - 0.000355295014225 * X2 + 2.216778544907194 * X3 + 0.005042239572897 * X4 - 0.046771152962135 * X5 + 4.330941544606418 * X1^2 - 0.000000745656814 * X2^2 - 31.582143858444198 * X3^2 - 0.000041427857404 * X4^2 + 0.000540239218776 * X5^2 + 0.006277898765933 * X1 * X2 - 53.349524139485816 * X1 * X3 - 0.012409597487409 * X1 * X4 - 0.340152093642835 * X1 * X5 - 0.000866340604559 * X2 * X3 + 0.000005209576702 * X2 * X4 + 0.000115555146264 * X2 * X5 + 0.006095282897997 * X3 * X4 + 0.236764117677313 * X3 * X5 + 0.000395941759427 * X4 * X5 \quad [12]$$

The above surrogate models are utilized to predict the maximum principal stress and the maximum principal strain in the transmission tower system under earthquakes. The surrogate models should be checked for reliability then be used to predict the system responses. By determining the coefficient of determination for both surrogate models denoted by R2, the reliability of each surrogate model is determined.

6.5 Coefficient of Determination

The construction of reliable surrogate models for the responses of the transmission tower system under earthquakes needs to calculate the coefficient of determination R2 through comparison process between the results of the numerical simulations and the surrogate models. The coefficient of determination for the maximum principal stress and maximum principal strain of the transmission tower are collected from numerical simulations of 25 models. The coefficient of determination for the maximum principal stress was R2 = 0.9706 (see Figure 10). It is obvious that there is 2.94% of the transmission tower system response is not recognized which is a very small portion which can be neglected approximately. This is an indication that the surrogate model is an excellent tool in predicting the structural system of the transmission tower under earthquakes.

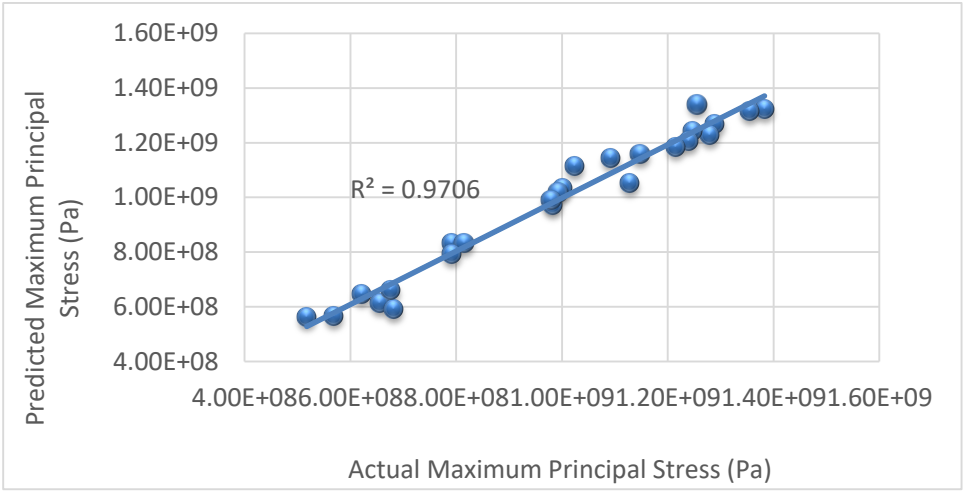

Figure 10: Coefficient of determination-maximum principal stress

The coefficient of determination for the maximum principal strain of the transmission tower system was $R^2 = 0.9278$ (see Figure 11). It is clear that there is only 7.22% of the response of the transmission tower system is not recognized which is a small fraction. This is an evidence that the surrogate model is excellent in predicting the behavior of the transmission tower system under the earthquakes.

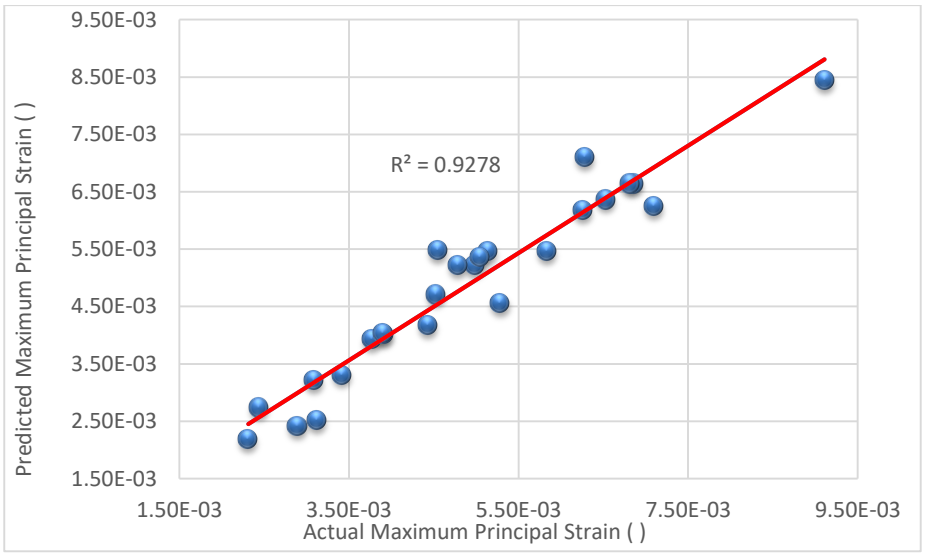

Figure 11: Coefficient of determination-maximum principal strain

7. Conclusions

We have concluded the following points from the results and the discussion:

1- The numerical simulation using ABAQUS program performed very well in simulating the behavior of the transmission tower system under different earthquakes. The accuracy of these results supports the surrogate modeling and the optimization stages.
2- The surrogate modeling manifested an excellent performance in representing the structural behavior of the transmission tower. It determined reliable predicted values for the maximum principal stress and maximum principal strain of the system under earthquakes.

3- The design of the transmission tower system under different earthquakes is easily and efficiently controlled supporting on the results of the surrogate modeling and the numerical simulations. Consequently, faster and safer design can be secured in addition to less cost for the design through the design stage and even after construction for existing weak designs of transmission tower systems.

References

Alam, M. J., & Santhakumar, A.R. (1996). Reliability analysis and full-scale testing of transmission tower. *Journal of Structural Engineering*, 122(3), 338-344.

American Society of Civil Engineers Task Committee on Tower Design. "Guide for design of steel transmission towers." American Society of Civil Engineers, 1971.

Diana, G., Yamasaki Y., Larsen A., Rocchi D., Giappino S., Argentini T., Pagani A., Villani M., Somaschini C., & Portentoso M. (2013). Construction stages of the long span suspension izmit bay bridge: Wind tunnel test assessment. *Journal of Wind Engineering & Industrial Aerodynamics*, 123, 300-310.

Khuri, A. I., & Mukhopadhyay S. (2010). Response surface methodology. *John Wiley & Sons, Inc. WIREs Computational Statistics*, 2(2), 128-149.

Kwak, J-S. (2005) Application of Taguchi and response surface methodologies for geometric error in surface grinding process. *Int J Mach Tools Manuf*, 45, 327–34.

Larsen, A., & Gimsing, N.J. (1992). Wind engineering aspects of the east bridge tender project. *Journal of Wind Engineering & Industrial Aerodynamics*, 42(1-3), 1405–1416.

Larsen, A., & Larose, G. L. (2015). Dynamic wind effects on suspension and cable-stayed bridges. *Journal of Sound and Vibration*, 334(1), 2–28.

Li, T., Ruisheng, M., Haiyang P., Canxing, Q., & Wenfeng, L. (2017). Progressive collapse analysis of long-span transmission tower-line system under multi-component seismic excitations. *Advances in Structural Engineering*, 20(12), 1920-1932.

Meng X. L., Guo Z. S, Ding Q. S., Zhu, L. D., (2011). Influence of wind fairing angle on vortex-induced vibrations and flutter performances of closed and semi-closed box decks. *Engineering Mechanics*, 28, 184-188.

Miyata, T. (2003). Historical view of long-span bridge aerodynamics. *Journal of Wind Engineering & Industrial Aerodynamics*, 91, 1393-1410.

Moon, B., Ji-Hun, P., Sung-Kyung, L., Jinkoo Kim, T. K., & Kyung-Won, M. (2009). Performance evaluation of a transmission tower by substructure test. *Journal of Constructional Steel Research*, *65*(1), 1-11.

Myers, R.H., Montgomery, D.C., Anderson-Cook, C.M. (2016). *Response surface methodology: Process and product optimization using designed experiments*. John Wiley & Sons.

Richardson, J.R. (1975). Advances in technique for determining the aero-elastic characteristics of suspension bridges.

Sham, S., & Wyatt, T. A. (2016). Construction aerodynamics of cable-stayed bridges for record spans: Stonecutters bridge. *Structures*, 8, 94-110.

Tang H., Zhang H., Mo W., & Li Y. (2021). Flutter Performance of Box Girders with Different Wind Fairings at Large Angles of Attack. *Wind and Structures*, 32: 509-520.

Walid, A., Latif, A., Ahmed, A. & Aziz, A. (2016). Aeroelastic investigation of long span suspension bridge decks by numerical cfd and fsi analyses. *Civil and Environmental Research*, 8(7), 81-90.

Wang, Q., Liao, H., Li, M., & Ma, C. (2012). Influence of aerodynamic shape of streamline box girder on bridge flutter and vortex-induced vibration. *Journal of Highway and Transportation Research and Development*, 29, 44-50.

Xiaohong, L., Wei, W., & Jian, F. (2018). Collapse analysis of transmission tower subjected to earthquake ground motion. *Modelling and Simulation in Engineering*, 2018, Article ID 2687561.